Manifold T-spline

Ying He, Kexiang Wang, Hongyu Wang, Xianfeng Gu, and Hong Qin

Center for Visual Computing (CVC) and Department of Computer Science
Stony Brook University, Stony Brook, NY, 11794-4400, USA
{yhe, kwang, wanghy, gu, qin}@cs.sunysb.edu

Abstract. This paper develops the manifold T-splines, which naturally extend the concept and the currently available algorithms/techniques of the popular planar tensor-product NURBS and T-splines to arbitrary manifold domain of any topological type. The key idea is the global conformal parameterization that intuitively induces a tensor-product structure with a finite number of zero points, and hence offering a natural mechanism for generalizing the tensor-product splines throughout the entire manifold. In our shape modeling framework, the manifold T-splines are globally well-defined except at a finite number of extraordinary points, without the need of any tedious trimming and patching work. We present an efficient algorithm to convert triangular meshes to manifold T-splines. Because of the natural, built-in hierarchy of T-splines, we can easily reconstruct a manifold T-spline surface of high-quality with LOD control and hierarchical structure.

1 Introduction

Despite many new shape representations proposed in recent years, to date, NURBS remain the prevailing industrial standard for surface modeling in CAD/CAM primarily because of their many attractive geometric properties and their dominant use in modeling and design software industry. Nevertheless, they exhibit two major shortcomings: (1) NURBS control points must always align themselves in a rectangular grid. As a result, localized details and sharp features can not be easily accommodated without introducing many more control points via knot insertion. Moreover, level-of-detail (LOD) control and hierarchical structure facilitating multiresolution analysis are impossible using a single-level NURBS; (2) due to the nature of its rectangular structure, a single NURBS surface can only represent very simple shapes such as open surfaces or tori. In practice, in order to modeling surfaces of complicated topology, one must define a network of tensor-product *B*-spline or NURBS patches and maintain certain continuity requirement between adjacent patches [1, 2]. Furthermore, surface trimming and abutting are oftentimes unavoidable.

To combat the above deficiencies of tensor-product NURBS, two recently developed techniques, T-spline [3] and manifold spline [4], have been introduced in shape modeling community. T-splines, developed by Sederberg, Zheng, Bakenov, and Nasri [3], are a generalization of NURBS surfaces that are capable of significantly reducing the number of superfluous control points by using the T-junction mechanism. The main difference between a T-spline control mesh and a NURBS control mesh is that T-splines

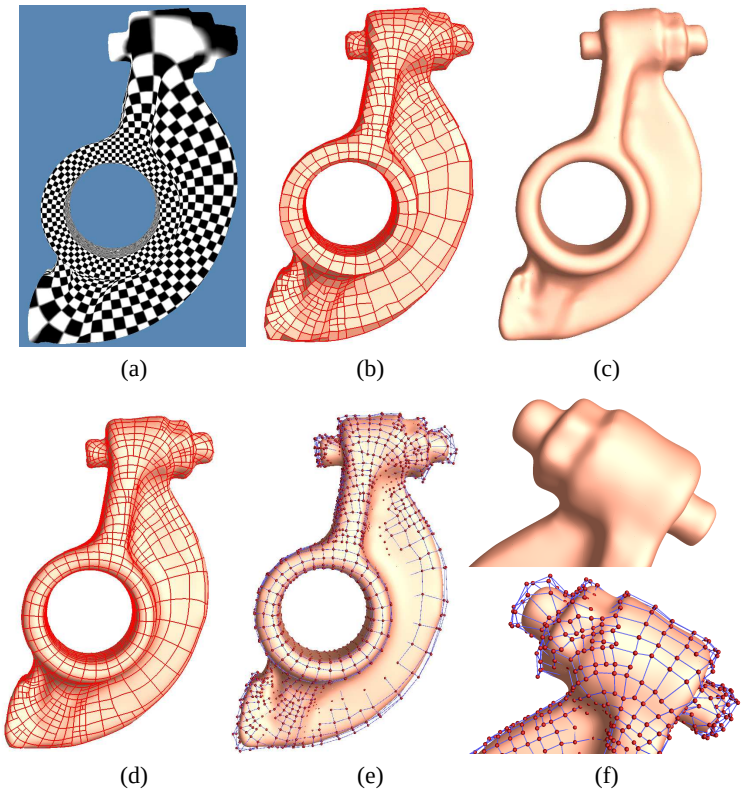

Fig. 1. Modeling the genus-one Rocker Arm model by manifold T-spline. (a) The conformal structure induces a natural curvilinear coordinate on the manifold domain. (b) Construct the domain manifold by tracing the iso-curves of the global conformal parameterization. Note that the domain manifold M contains only quadrilaterals and T-junctions. (c) A cubic (C^2-continuous) manifold T-spline surface. (d) The red curves on the manifold T-spline surface are the images of the edges on the domain manifold along the u and v directions. (e) $2,121$ control points are highlighted. (f) The close-up view of the details.

allow a row or column of control points to terminate at anywhere without strictly enforcing the rectangular grid structure throughout the parametric domain. Consequently, T-splines enable much better local refinement capabilities than NURBS. Furthermore, using the techniques presented in [3], it is possible to merge adjoining T-spline surfaces into a single T-spline without adding new control points. However, this patching process requires that the knot intervals of the to-be-merged edges must establish an one-to-one correspondence between the two surfaces.

Manifold spline, presented by Gu, He, and Qin [4], is a general theoretical framework, in which the existing spline schemes defined over planar domains can be systematically generalized to any manifold domain of arbitrary topology (with or without boundaries) using affine structures. They demonstrated the idea of manifold spline only using triangular B-splines because of the attractive properties of triangular B-splines,

such as arbitrary triangulation, parametric affine invariance, and piecewise polynomial reproduction. Despite the generality of triangular *B*-splines, they have not been used in an industrial setting due to their modeling complexity in evaluation, differential property computation, and data management. In practice, 2D-array-like control point layout facilitates the effective computation, shape analysis, and perhaps above all, the simplicity of data structure. In spite of all the potential modeling power associated with our manifold spline, its has not gained a widespread popularity mainly due to the fact that its constituent is triangular *B*-spline. To further promote its utility in real-world applications, we must bring tensor-product splines such as NURBS into our manifold spline framework and demonstrate its efficacy. Our current research reported here aims to serve this need.

In particular, this paper presents the manifold T-splines, a natural and necessary integration of T-splines and manifold splines, with a goal to retain all the desirable properties while overcoming the aforementioned modeling drawbacks at the same time. Manifold T-splines can be directly defined over the manifold of arbitrary topology to accurately represent various shapes with complicated geometry and topology. Manifold T-splines naturally inherit all the attractive properties from T-splines defined over a planar domain, including the powerful local refinement capabilities and the hierarchical organization for LOD control. Definitely worth mentioning here is that its building block comes from tensor-product NURBS, an industrial standard in all CAD/CAM software systems with a large variety of algorithmic routines available. The systematic development of our manifold T-splines streamlines the entire process of our manifold splines by demonstrating the intrinsic connection between manifold splines and popular tensor-product NURBS. As a result, our manifold T-splines are suitable for both expert users and novice users. Users, who are familiar with NURBS, can easily embrace our manifold T-splines without extra difficulties, as all the software routines and existing algorithms for tensor-product NURBS remain unchanged in our new modeling framework. Figure 1 shows the manifold T-spline of genus-one Rocker Arm model. This manifold T-spline is a single spline representation without any trimming, cutting and patching work.

2 Previous Work

2.1 Hierarchical Splines and B-splines/Bézier Splines Based Modeling Techniques

Forsey and Bartels presented the hierarchical *B*-spline [5], in which a single control point can be inserted without propagating an entire row or column of control points. Gonzalez-Ochoa and Peters [6] presented the localized-hierarchy surface splines which extended the hierarchical spline paradigm to surfaces of arbitrary topology. Yvart *et al* presented the G^1 hierarchical triangular spline which works on any 2-manifold triangular mesh of arbitrary genus and has no restriction on the connectivity of the vertices. They demonstrated hierarchical triangular splines in smooth adaptive fitting of 3D models in [7]. In [3], Sederberg *et al.* presented the T-spline, a generalization of the non-uniform B-spline surfaces. T-spline control grids need not to be totally regular. In particular, they allow T-junctions, and lines of control points need not to traverse

the entire control grid. Therefore, T-splines enable true local refinement without introducing additional, unnecessary control point in nearby regions. Sederberg *et al.* also developed an algorithm to convert NURBS surfaces into T-spline surfaces, in which a large percentage of superfluous control points are eliminated [8].

There also exist large number of literatures in modeling 3D shapes of complicated topology using *B*-splines and Bézier patches. Due to the space limitation, we just name a few of them. Peters constructed C^1 surfaces of arbitrary topology using biquadratic and bicubic spliens [9]. This method generalizes the standard biquadratic tensor-product *B*-spline representation to irregular meshes, i.e., there are no regularity restrictions on the input meshes. Hahmann and Bonneau [10] presented a method for interpolating 2-manifold triangular meshes with a parametric surface composed of Béizer patches of degree 5. This method can generate visually pleasing shapes without the unwanted undulations, even if the interpolated mesh has irregular features. Loop and DeRose presented a method for constructing surfaces from control meshes of arbitrary topological type [11]. This method is based on S-patches which generalize biquadratic and bicubic B-splines. The above *B*-splines and Bézier spline based methods share one common property: they require the control points along the boundaries of adjacent spline patches satisfying certain constraints to reach G^1, C^1 or C^2 continuity. Therefore, only part of the control points serve the geometric modeling purpose.

2.2 Manifold Construction

There are some related work on defining functions over manifold. In essence, manifold construction is different from the above work on splines of arbitrary topology. The shape (2-manifold) is covered by several charts. One builds functions on each chart. Due to certain continuity requirement of the transition functions between overlapping charts, the smoothness properties of the manifold functions are *automatically* guaranteed. Therefore, there are no restrictions/constraints on the control points. All the control points are free variables in the entire modeling process. Furthermore, manifold constructions can generate C^k smooth surfaces.

Grimm and Hugues [12] pioneered a generic method to extend B-splines to surfaces of arbitrary topology, based on the concept of overlapping charts. Cotrina *et al.* proposed a C^k construction on manifold [13, 14]. Ying and Zorin [15] presented a manifold-based smooth surface construction method which has C^∞-continuous with explicit nonsingular parameterizations only in the vicinity of regions of interest.

More recently, Gu *et al.* [4] developed a general theoretical framework of manifold splines in which spline surfaces defined over planar domains can be systematically generalized to any manifold domain of arbitrary topology (with or without boundaries). Manifold spline is different from the above manifold construction methods in the following aspects: 1) The transition functions of manifold spline must be affine. Therefore, the requirements of manifold spline is much stronger than previous work. That is why topological obstruction plays an important role in the construction. 2) Manifold spline produces either polynomial or rational polynomials. On any chart, the basis functions are always polynomials or rational polynomials, and represented as *B*-splines or rational *B*-splines.

To further improve our manifold spline results, in this paper we develop the manifold T-spline, which combine the benefits of our manifold spline and T-spline towards a more practical solution on surface modeling and simulation.

3 Manifold T-spline

As pointed out in [4], if a particular planar spline scheme is invariant under the parametric affine transformation, it can be generalized to manifold domain of arbitrary topology with no more than Euler number of singular points. For example, triangular *B*-splines and Powell-Sabin splines have been generalized from the planar domain to manifold of arbitrary topology [4, 16].

T-splines [3] are a generalization of NURBS surfaces that are capable of significantly reducing the number of superfluous control points. T-splines are parametric affine invariant, and therefore, they can be generalized to manifold domain without theoretical difficulties. The overview of the construction algorithm is as follows:

Algorithm: Construction of manifold T-spline
Input: A polygonal mesh P, maximal fitting tolerance ε
Output: A manifold T-spline F which approximates P

1. Compute the global conformal parameterization of P.
2. Construct the domain manifold M (a coarse T-mesh) according to the conformal structure of P.
3. Assign the knot interval for each edge of M to get the initial T-spline F.
4. Compute the control points of F by minimizing a linear combination of the interpolation and fairness functional.
5. Locally refine the T-spline F if the fitting error is bigger than the user specified fitting tolerance ε and repeat step 4. Otherwise, output F.

3.1 Global Conformal Parameterization

Suppose P is a surface with handles, either open or closed. A global conformal parameterization is a map $\phi : P \to \mathbb{R}^2$, such that each point p on M is mapped to a point on the planar parametric domain $\phi(p) = (u(p), v(p))$. Furthermore, the map ϕ is angle preserving, which is equivalent to the following fact: suppose we arbitrarily draw two intersecting curves γ_1, γ_2 on M, the intersection angle is α, then the intersection angle of their images $\phi(\gamma_1)$ and $\phi(\gamma_2)$ is also α. Mathematically, the conformality of the parameterization is formulated in the following way: the first fundamental form of M under conformal parameterization (u,v) is represented as $ds^2 = \lambda^2(u,v)(du^2 + dv^2)$, where λ is called the conformal factor, which indicates the area ratio between the area on M and that on the plane.

In practice, it is more convenient to compute the gradient fields of ϕ, namely $(\bigtriangledown u, \bigtriangledown v)$. If ϕ is conformal, then it satisfies the following criteria:

$$\bigtriangledown v(p) = \mathbf{n}(p) \times \bigtriangledown u(p),$$

where $\mathbf{n}(p)$ is the normal at the point p, also

$$\bigtriangledown \times \bigtriangledown u = \bigtriangledown \times \bigtriangledown v = 0,$$

because the gradient fields are curl-free. Formally, a pair of vector fields satisfying the above conditions is a *holomorphic 1-form*. There exists an infinite number of this kind of vector fields. They form a $2g$ dimensional real linear space, where g is the number of handles of P.The integration curves $\bigtriangledown u$ and $\bigtriangledown v$ are called *horizontal and vertical trajectories*, respectively. It is obvious that the horizontal and vertical trajectories are orthogonal everywhere and two horizontal (vertical) trajectories do not intersect each other in general. There are special points on P, where two horizontal trajectories intersect (two vertical trajectories also intersect). It can be proven that, at those points, the conformal factors are zero, therefore, such kind of points are called *zero points* of the holomorphic 1-form. By the Poincaré-Hopf theorem, every vector field on a closed surface of genus $g \neq 1$ must have zero points. The holomorphic 1-form has the unique property that it has the minimal number of zero points, i.e., $|2g-2|$ zero points.

The following theorem reveals the relationship between the conformal structure and the affine structure.

Theorem 1. ([4]) *Given a closed genus g surface M, and a holomorphic 1-form ω. Denote by $Z = \{zeros\ of\ \omega\}$ the zero points of ω. Then the size of Z is no more than $2g-2$, and there exists an affine atlas on M/Z deduced by ω.*

Essentially, Theorem 3 indicates that an affine atlas of a manifold M can be deduced from its conformal structure in a straightforward fashion.

3.2 Domain Manifold Construction

Unlike the manifold triangular *B*-spline which does not have any restriction on the domain manifold [4], manifold T-splines require that the domain manifold has mainly rectangular structure possibly with T-junctions. The global conformal parameterization induces the natural tensor-product structures on the domain manifold with Euler number of zero points, which furthermore induces the affine structure of the domain manifold. In the subsection, we present the method to construct the domain manifold (quad mesh with T-junctions). The method varies different types of surfaces. We explain the details for each case: genus zero closed surfaces, genus one closed surfaces, high genus closed surfaces and surfaces with boundaries.

Genus zero closed surfaces Every genus zero closed surface P can be conformally mapped to a sphere. Practical algorithms for computing such maps are given in [17, 18]. The idea used in [17] is that, for genus zero closed surfaces, conformal maps are equivalent to harmonic maps, which can be computed using heat flow method. Denote by $f : P \to \mathbb{S}^2$ the conformal map and (θ, ϕ) the spherical coordinates. The horizontal trajectories on P are the curves $f^{-1}(\phi = const.)$, and the vertical trajectories are $f^{-1}(\theta = const.)$. The preimages of the north and south poles are the zero points. The trajectories are orthogonal everywhere except at the zero points and form the conformal net. Figure 8 shows the conformal parameterization and the domain manifold of the genus zero Iphegenia model.

Genus one closed surfaces The holomorphic 1-form ω on a genus one closed surface P is nonsingular everywhere, i.e., there are no zero points. Thus, the construction

of domain manifold is straightforward. By integrating ω on P, the whole surface can be conformally mapped to a parallelogram on the plane, called the *fundamental period* of P. In general, this is not a rectangle, but a skewed parallelogram whose shape is determined by the conformal structure of P. If the fundamental period is a rectangle, then all the horizontal and vertical trajectories forming the conformal net on the surfaces are closed circles. Otherwise, two families of curves parallel to the sides of the parallelogram are used as the trajectories. Figure 1 shows the conformal parameterization and domain manifold of the Rocker Arm model.

High genus closed surfaces The global structure of conformal nets on high genus closed surfaces is more complicated than the above cases due to the existence of zero points.

Once the differential form is obtained, we locate all its zero points and all the horizontal trajectories passing through them, namely, the *critical horizontal trajectories*. The critical horizontal trajectories partition the surface into several patches. Each patch is either a cylinder or a disk. All patches can be conformally mapped to a planar rectangle. Therefore, we can build the conformal net for each patch, and glue them together. Note that, the T-junctions are allowed along the boundaries of the patches. The zero points, the critical horizontal trajectories, and the patches form a graph, the so called *critical graph*.

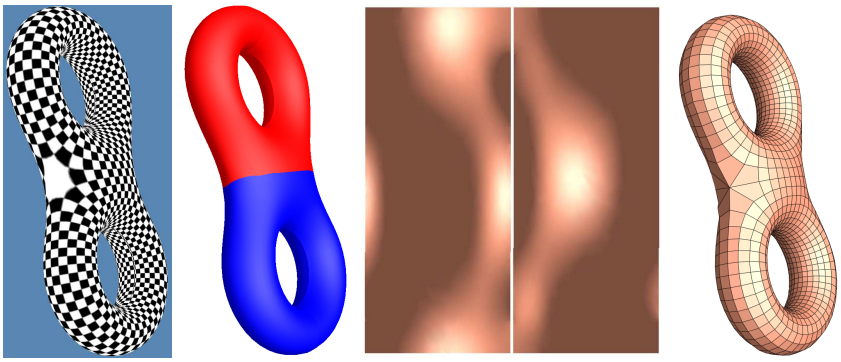

Fig. 2. Critical graph of the two-hole torus model. (a) Global conformal parameterization. (b) The critical horizontal trajectories partition the surface into two patches. Each patch is a cylinder. (c) Map each patch to a planar rectangle. (d) We build the quad mesh for each patch and then glue them together.

Surfaces with boundaries For surface with boundaries, we need to double cover the original surfaces to make it become a closed surface (see [19] for the details of double covering technique). Generally, if P is of genus g and has b boundaries, then the double-covered surface $\bar{P}$ is a closed surface with genus $2g+b-1$. We compute the holomorphic 1-form basis of $\bar{P}$ and then find a special holomorphic 1-form $\omega = (\omega_u, \omega_v)$ on it such that ω_u is orthogonal to ∂P everywhere. This ω induces a conformal net on P

for which all curves in ∂P are vertical trajectories. Figure 6 illustrates the critical graph of the Stanford Bunny. In order to get the uniform global conformal parameterization, three cuts are introduced in the original model, two are at the tips of ears, one is at the bottom. Therefore, it is topologically equivalent to a 2-hole disk. The double covered surface is of genus 2. The zero point is between the roots of the two ears. The critical horizontal trajectories partition the surface into 2 connected components, each component is a topological disk which can be conformally mapped to a rectangle in the plane by integrating the holomorphic 1-form ω. Then the domain manifold can be constructed by remeshing each component.

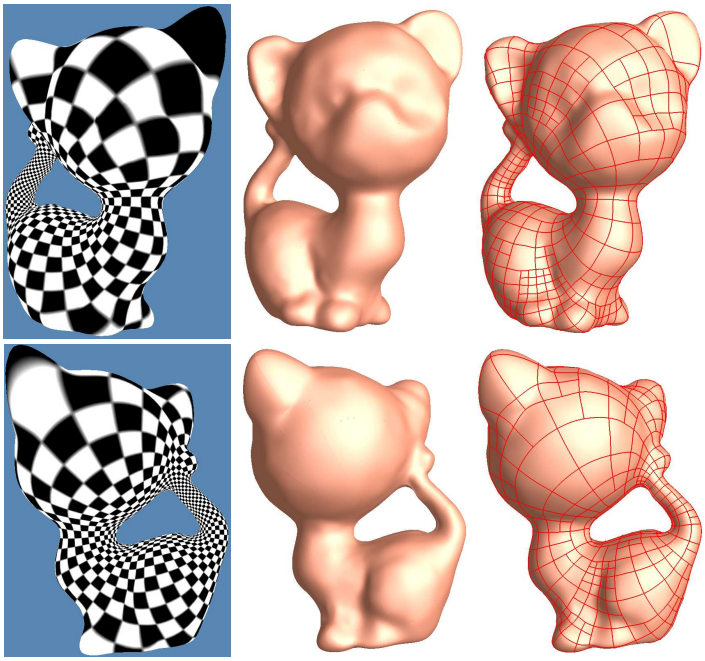

Fig. 3. Modeling the Kitten model using manifold T-spline with 765 control points.

3.3 Hierarchical Surface Reconstruction

Given the domain manifold M with conformal structure $\phi : M \to \mathbb{R}^2$, the manifold T-spline can be formulated as follows:

$$\mathbf{F}(\mathbf{u}) = \sum_{i=1}^{n} \mathbf{C}_i B_i(\phi(\mathbf{u})),\ \mathbf{u} \in M, \tag{1}$$

where B_is are basis functions and $\mathbf{C}_i = (x_i, y_i, z_i, w_i)$ are control points in $\mathbb{P}^4$ whose weights are w_i, and whose Cartesian coordinates are $\frac{1}{w_i}(x_i, y_i, z_i)$. The cartesian coordi-

nates of points on the surface are given by

$$\frac{\sum_{i=1}^{n}(x_i,y_i,z_i)B_i(\phi(\mathbf{u}))}{\sum_{i=1}^{n}w_iB_i(\phi(\mathbf{u}))}. \tag{2}$$

Given a parameter $\mathbf{u} \in M$, the evaluation can be carried out on arbitrary charts covering $\mathbf{u}$.

We now discuss the problem of finding a good approximation of a given polygonal mesh P with vertices $\{\mathbf{p}_i\}_{i=1}^{m}$ by a manifold T-spline.

A commonly-used technology is to minimize a linear combination of interpolation and fairness functionals, i.e.,

$$\min E = E_{dist} + \lambda E_{fair}. \tag{3}$$

The first part is

$$E_{dist} = \sum_{i=1}^{m} \|\mathbf{F}(\mathbf{u}_i) - \mathbf{p}_i\|^2$$

where $\mathbf{u}_i \in M$ is the parameter for $\mathbf{p}_i$, $i = 1,\ldots,m$.
The second part E_{fair} in (3) is a smoothing term. A frequently-used example is the thin-plate energy,

$$E_{fair} = \iint_M (\mathbf{F}_{uu}^2 + 2\mathbf{F}_{uv}^2 + \mathbf{F}_{vv}^2)dudv.$$

Note that both parts are quadratic functions of the unknown control points.

We solve Equation 3 for unknown control points using Conjugate Gradient method. The value and gradient of the interpolation functional and fairness functional can be computed straightforwardly.

In our method, we control the quality of the manifold T-spline spline by specifying the maximal fitting tolerance $L_\infty = \max \|\mathbf{F}(\mathbf{u}_i) - \mathbf{p}_i\|$, $i = 1,\ldots,m$. If the current surface does not satisfy this criterion, we employ adaptive refinement to introduce new degrees of freedom into the surface representation to improve the fitting quality. Because of the natural and elegant hierarchial structure of T-splines, this step can be done easily. Suppose a domain rectangle I violates the criterion and denote L_∞^I the L_∞ error on rectangle I. If the $L_\infty^I > 2\varepsilon$, split the rectangle I using 1-to-4 scheme; Otherwise, we divide I into two rectangles by splitting the longest edge.

After adaptive refinement, we then re-calculate the control points until the maximal fitting tolerance is satisfied. Figure 3.3 shows the whole procedure of hierarchical fitting of the David's head model. The initial spline contains only 105 control points and the maximal error $L_\infty = 8.6\%$. Through six iterations, we can obtain a much more refined spline with 7706 control points. The maximal fitting error reduces to 0.74%. As shown in the close-up view (Figure 5), our hierarchical data fitting procedure can produce high quality manifold T-splines with high-fidelity recovered details.

3.4 Experimental Results

We have implemented a prototype system on a 3GHz Pentium IV PC with 1GB RAM. We perform experiments on various real-world surfaces. In order to compare the fitting quality across different models, we uniformly scale the models to fit within a unit

Table 1. Statistics of test cases. N_p, # of points in the polygonal mesh; N_c, # of control points; *rms*, root-mean-square error; L_∞, maximal error. The execution time measures in minutes.

Object	N_p	N_c	*rms*	L_∞	Time
David	200,000	7,706	0.08%	0.74%	39m
Bunny	34,000	1,304	0.09%	0.81%	18m
Iphegenia	150,000	9,907	0.06%	0.46%	53m
Rocker Arm	50,000	2,121	0.04%	0.36%	26m
Kitten	40,000	765	0.05%	0.44%	12m

cube. Table 1 summarizes the spline complexities and performance. The execution time includes the global conformal parameterization, domain manifold construction and hierarchical spline fitting. Figure 8 shows the manifold T-spline of Iphegenia model. Note that the details can be reconstructed easily with an appropriate number of control points.

4 Conclusions

In this paper, we have presented the manifold T-splines as a novel shape modeling paradigm for complicated geometry and topology. Built upon our previous work, the manifold T-splines integrate the algorithms and techniques of the widely-used, tensor-product NURBS and recently-proposed T-splines towards the effective shape modeling for arbitrary manifold. Our motivations come from two frontiers: (1) extending NURBS and T-splines to the manifold setting; and (2) promoting the widespread acceptance of manifold splines in real-world, shape modeling applications. The central idea is the global conformal parameterization that naturally induces a tensor-product structure over arbitrarily complicated manifold. In our shape modeling framework, the manifold T-splines are globally well-defined except at a finite number of extraordinary points without the need of any tedious and counter-intuitive trimming and patching work. Driven by the theoretical advances, we have developed an efficient algorithm automatically construct manifold T-splines from input data points. The salient features of our manifold T-splines include: natural hierarchical structure, local refinement, LOD control, tensor-product splines as building blocks, etc. Our new techniques are poised to be effective in shape modeling, and interactive design.

Acknowledgements

This work was supported in part by the NSF grants IIS-0082035 and IIS-0097646, and an Alfred P. Sloan Fellowship to H. Qin and the NSF CAREER Award CCF-0448339 to X. Gu. The models are courtesy of Leif Kobbelt, Cyberware, Stanford University.

References

1. Eck, M., Hoppe, H.: Automatic reconstruction of b-spline surfaces of arbitrary topological type. In: Proceedings of SIGGRAPH 96. (1996) 325–334

2. Krishnamurthy, V., Levoy, M.: Fitting smooth surfaces to dense polygon meshes. In: Proceedings of SIGGRAPH 96. (1996) 313–324
3. Sederberg, T.W., Zheng, J., Bakenov, A., Nasri, A.H.: T-splines and t-nurccs. ACM Trans. Graph. **22** (2003) 477–484
4. Gu, X., He, Y., Qin, H.: Manifold splines. In: Proceedings of ACM Symposium on Solid and Physical Modeling (SPM '05). (2005) 27–38
5. Forsey, D.R., Bartels, R.H.: Hierarchical b-spline refinement. In: SIGGRAPH '88: Proceedings of the 15th annual conference on Computer graphics and interactive techniques, New York, NY, USA, ACM Press (1988) 205–212
6. Gonzalez-Ochoa, C., Peters, J.: Localized-hierarchy surface splines (less). In: SI3D '99: Proceedings of the 1999 symposium on Interactive 3D graphics, New York, NY, USA, ACM Press (1999) 7–15
7. Yvart, A., Hahmann, S., Bonneau, G.P.: Smooth adaptive fitting of 3d models using hierarchical triangular splines. In: SMI '05: Proceedings of the International Conference on Shape Modeling and Applications 2005 (SMI' 05). (2005) 13–22
8. Sederberg, T.W., Cardon, D.L., Finnigan, G.T., North, N.S., Zheng, J., Lyche, T.: T-spline simplification and local refinement. ACM Trans. Graph. **23** (2004) 276–283
9. Peters, J.: Surfaces of arbitrary topology constructed from biquadratics and bicubics. In: Designing fair curves and surfaces. SIAM (1994) 277–293
10. Hahmann, S., Bonneau, G.P.: Polynomial surfaces interpolating arbitrary triangulations. IEEE Transactions on Visualization and Computer Graphics **9** (2003) 99–109
11. Loop, C.: Smooth spline surfaces over irregular meshes. In: SIGGRAPH '94: Proceedings of the 21st annual conference on Computer graphics and interactive techniques. (1994) 303–310
12. Grimm, C., Hughes, J.F.: Modeling surfaces of arbitrary topology using manifolds. In: SIGGRAPH. (1995) 359–368
13. Cotrina, J., Pla, N.: Modeling surfaces from meshes of arbitrary topology. Computer Aided Geometric Design **17** (2000) 643–671
14. Cotrina, J., Pla, N., Vigo, M.: A generic approach to free form surface generation. In: SMA '02: Proceedings of the seventh ACM symposium on Solid modeling and applications. (2002) 35–44
15. Ying, L., Zorin, D.: A simple manifold-based construction of surfaces of arbitrary smoothness. ACM Trans. Graph. **23** (2004) 271–275
16. He, Y., Jin, M., Gu, X., Qin, H.: A C^1 globally interpolatory spline of arbitrary topology. In: Proceedings of the 3rd IEEE Workshop on Variational, Geometric and Level Set Methods in Computer Vision. Volume 3752 of Lecture Notes in Computer Science. (2005) 295–306
17. Gu, X., Wang, Y., Chan, T., Thompson, P., Yau, S.T.: Genus zero surface conformal mapping and its application to brain surface mapping. IEEE Transactions on Medical Imaging **23** (2004) 949–958
18. Gotsman, C., Gu, X., Sheffer, A.: Fundamentals of spherical parameterization for 3d meshes. Proceedings of SIGGRAPH 03 (2003) 358–363
19. Gu, X., Yau, S.T.: Global conformal surface parameterization. In: Proceedings of the Eurographics/ACM SIGGRAPH symposium on Geometry processing (SGP '03). (2003) 127–137

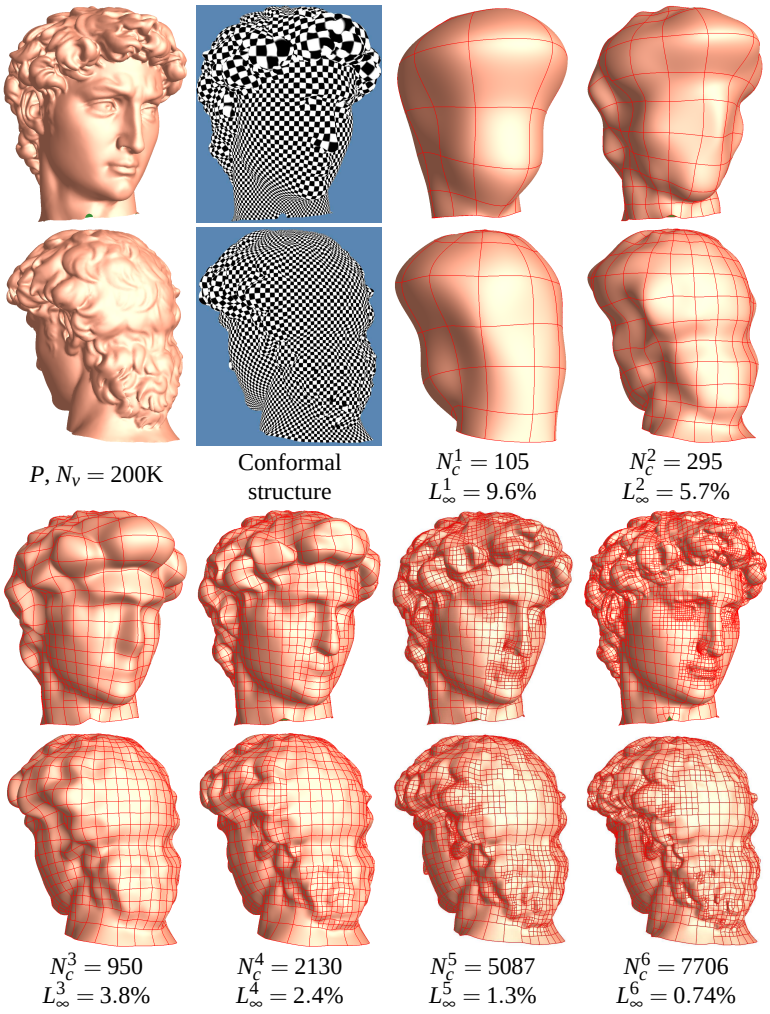

Fig. 4. Hierarchical surface reconstruction. N_c^i and L_∞^i are the number of control points and maximal fitting error in iteration i. N_v is the number vertices in the input polygonal mesh P. The input data is normalized to a unit cube.

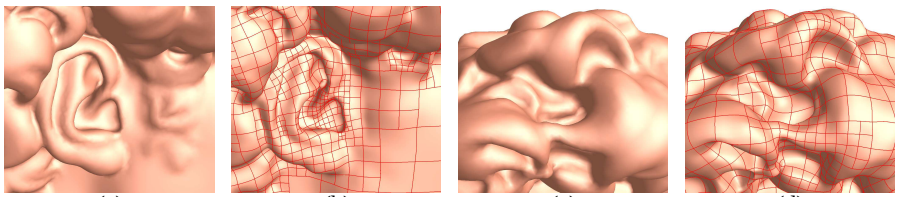

Fig. 5. Close-up of the reconstructed details. (a),(c) The original polygonal mesh. (b),(d) Manifold T-spline where the red curves highlight the T-junctions.

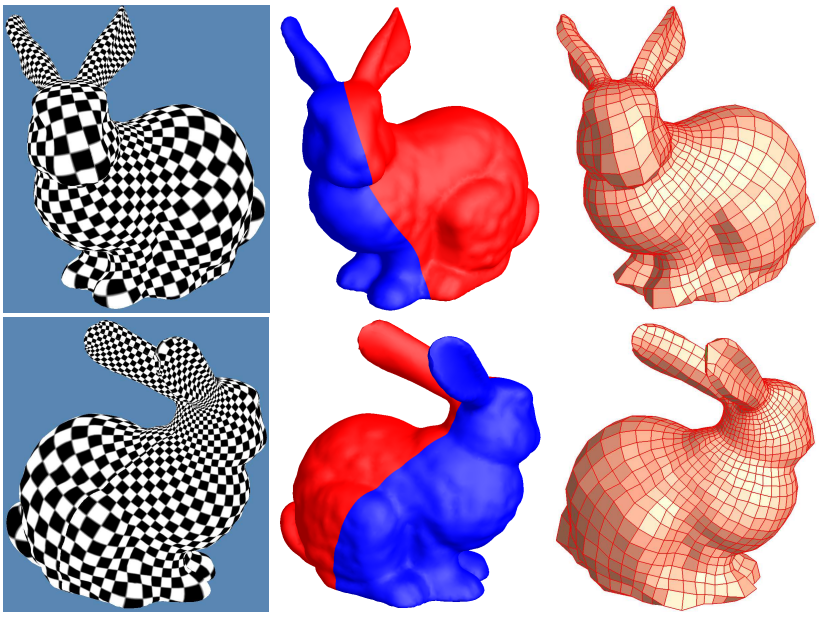

(a) (b) (c)

Fig. 6. Critical graph and domain manifold. (a) shows the global conformal parameterization. (b) shows the critical horizontal trajectories partition the whole surface into two components. Each component can be conformally mapped to a rectangle. (c) Construct the domain manifold (quad mesh with T-junctions) by remeshing each component. T-junctions are allowed along the critical trajectories.

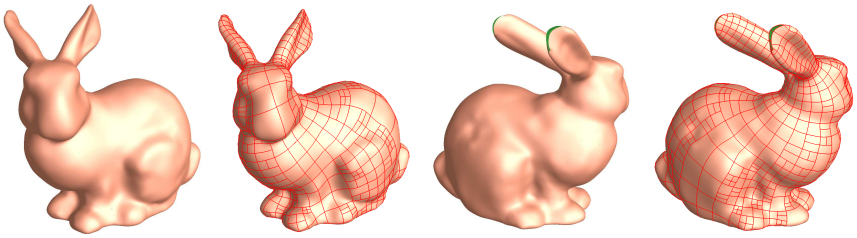

(a) (b) (c) (d)

Fig. 7. Converting Stanford Bunny into a manifold T-spline. (a)&(b) The front view. (c)&(d) The back view. The red curves illustrate the T-junctions on the spline surface.

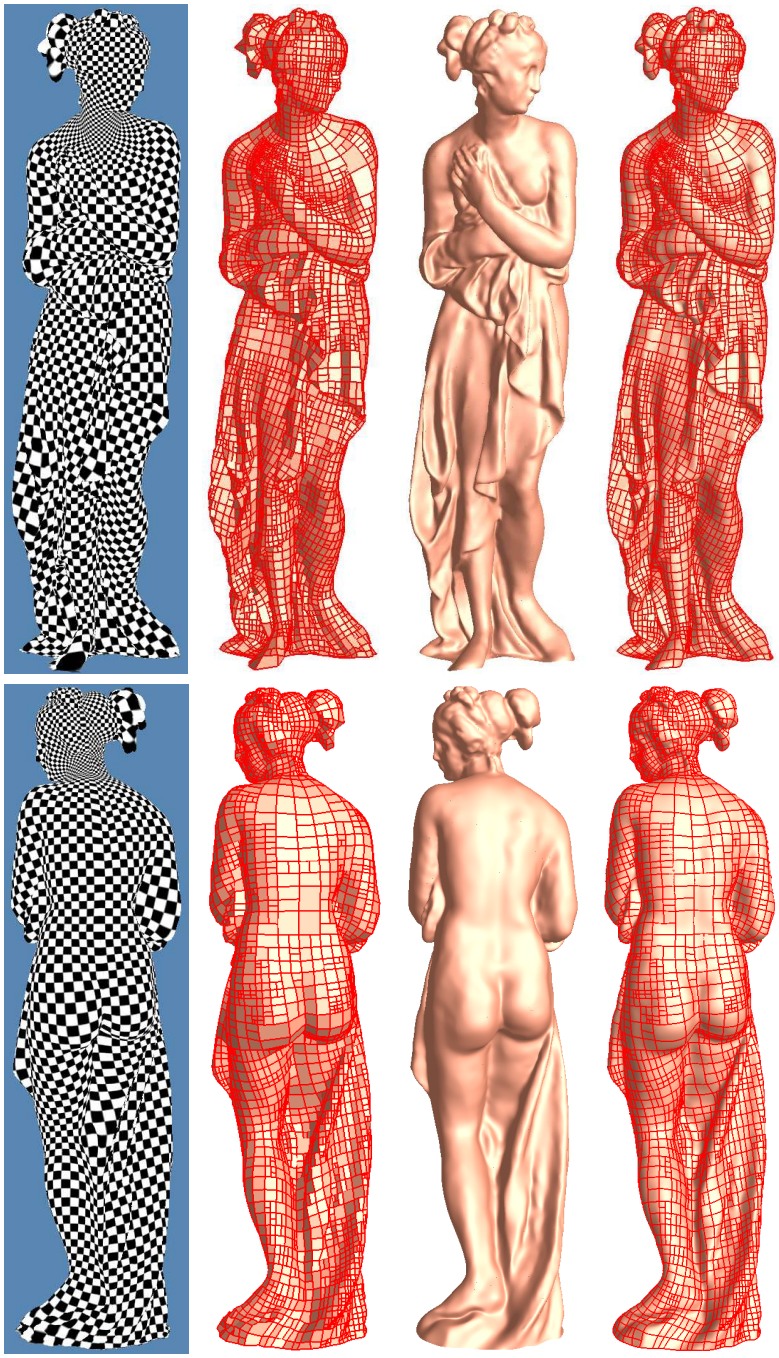

Fig. 8. Modeling the Iphegenia model using manifold T-spline. (a) Global conformal parameterization; (b) The domain manifold; (c) A C^2 manifold T-spline with $9,907$ control points; (d) The red curves are the images of the edges of the rectangles in the domain manifold.